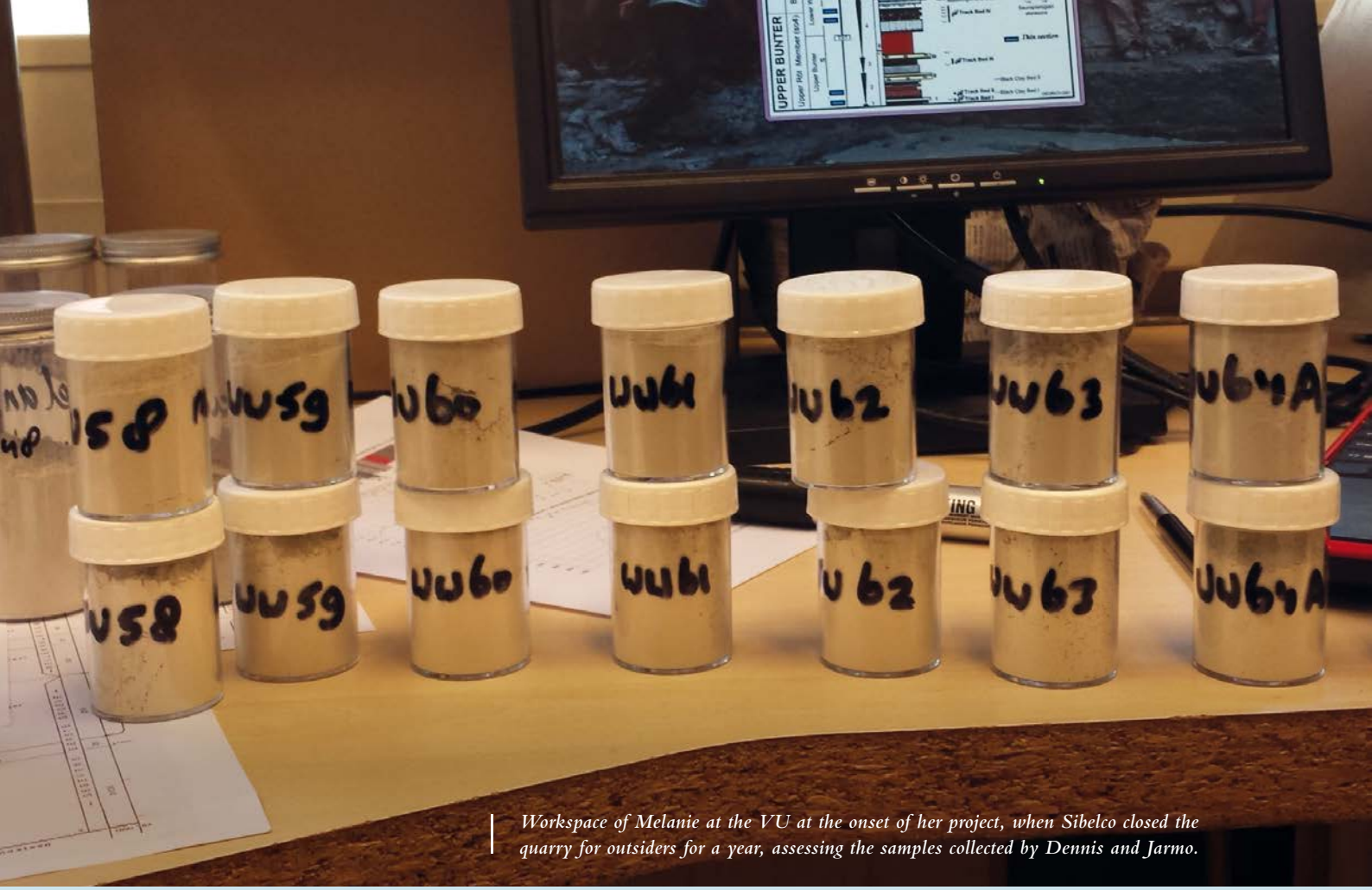

Workspace of Melanie at the VU at the onset of her project, when Sibelco closed the quarry for outsiders for a year, assessing the samples collected by Dennis and Jarmo.

Stratigraphy and Geochemistry of the Vossenveld Formation

U vindt een samenvatting aan het eind van de tekst.

Melanie A.D. During[1,2,4,]
Corresponding author:
palaeomelanie@gmail.com
Jarmo Pietersen[2,3,]
Dennis F.A.E. Voeten[1,2,6,]
Mehrdad Sardar Abadi[5,]
Suzan Verdegaal-Warmerdam[2,]
Anne S. Schulp[1,6,7,]
Jan Smit[2] ,
John J.G. Reijmer[2,8,]
Jeroen (H) J.L. van der Lubbe[1,2]

[1]Workgroup Muschelkalk Winterswijk, Dutch Geological Society, the Netherlands;

[2]Vrije Universiteit, Amsterdam, the Netherlands;

[3]Wiertsema & Partners, Tolbert, the Netherlands;

[4]Evolutionary Biology Center, Uppsala University, Uppsala, Sweden;

[5]School of Geolosciences, University of Oklahoma, Norman, USA;

[6]Naturalis Biodiversity Center, Leiden, the Netherlands;

[7]Utrecht University, Utrecht, the Netherlands;

[8]King Fahd University of Petroleum & Minerals, College of Petroleum Engineering & Geosciences, Dharan, Saudi Arabia;

Abstract | The Winterswijkse Steengroeve quarry complex in the east of the Netherlands exposes a ~ 40 m thick sedimentary sequence of intertidal and shallow marine deposits of the Vossenveld Formation dated as Anisian (early Middle Triassic). Here, we present a detailed stratigraphic and sedimentological description combined with geochemical data (carbonate content, spectral gamma ray, magnetic susceptibility, stable isotopes) of the sedimentary sequence in the Winterswijkse Steengroeve. Stable isotope ratios point to paleotemperatures in the range of 25 to 35 °C. These high temperatures in combination with the shallow enclosed character and proximity to the equator made the environment particularly susceptible to substantial evaporation and likely very saline. The concentration of predominantly isolated skeletal fossils resulted from storm activity. Unexpected is the overall increasing salinity in combination with the occurrence of larger sauropterygians in the top 10 m, accompanied by the halophytic bivalve *Neoschizodus orbicularis*. A subsequent literature study of the distribution of the sauropterygian genera described from the Vossenveld Formation sheds light on their deposition and burial conditions. The combined isotopic, geochemical, and sedimentological study on the Vossenveld Formation elucidates the depositional environment in which the rich fossil assemblage of Winterswijk is preserved. The obtained information on the preservation and paleoenvironment is pivotal in understanding the mode and pacing of the biotic recovery after the end-Permian mass extinction.

Introduction

The Winterswijkse Steengroeve quarry complex exposes a ~ 40 m thick sedimentary sequence comprised of intertidal and shallow marine strata of the Vossenveld Formation (Hagdorn & Simons, 2010) that dates to the Anisian (early Middle Triassic). The Anisian stage started only ~6 million years after the end-Permian extinction event, which accounts for the largest mass extinction in the history of life on Earth that caused the extinction of 96% of marine species and 72% of marine genera (Penn *et al.*, 2018). The global paleogeographic configuration during the Early Triassic involved a single supercontinent, Pangea, surrounded by the large Tethys Ocean (Ziegler, 1999). As Pangea broke up under the influence of tectonic activity in the Early Triassic, a semi-enclosed supracontinental basin formed in Central Europe (Ziegler, 1999). During the early Middle Triassic, this so-called Germanic Basin attained hydrological connection with the Tethys Ocean and was gradually flooded from east to west

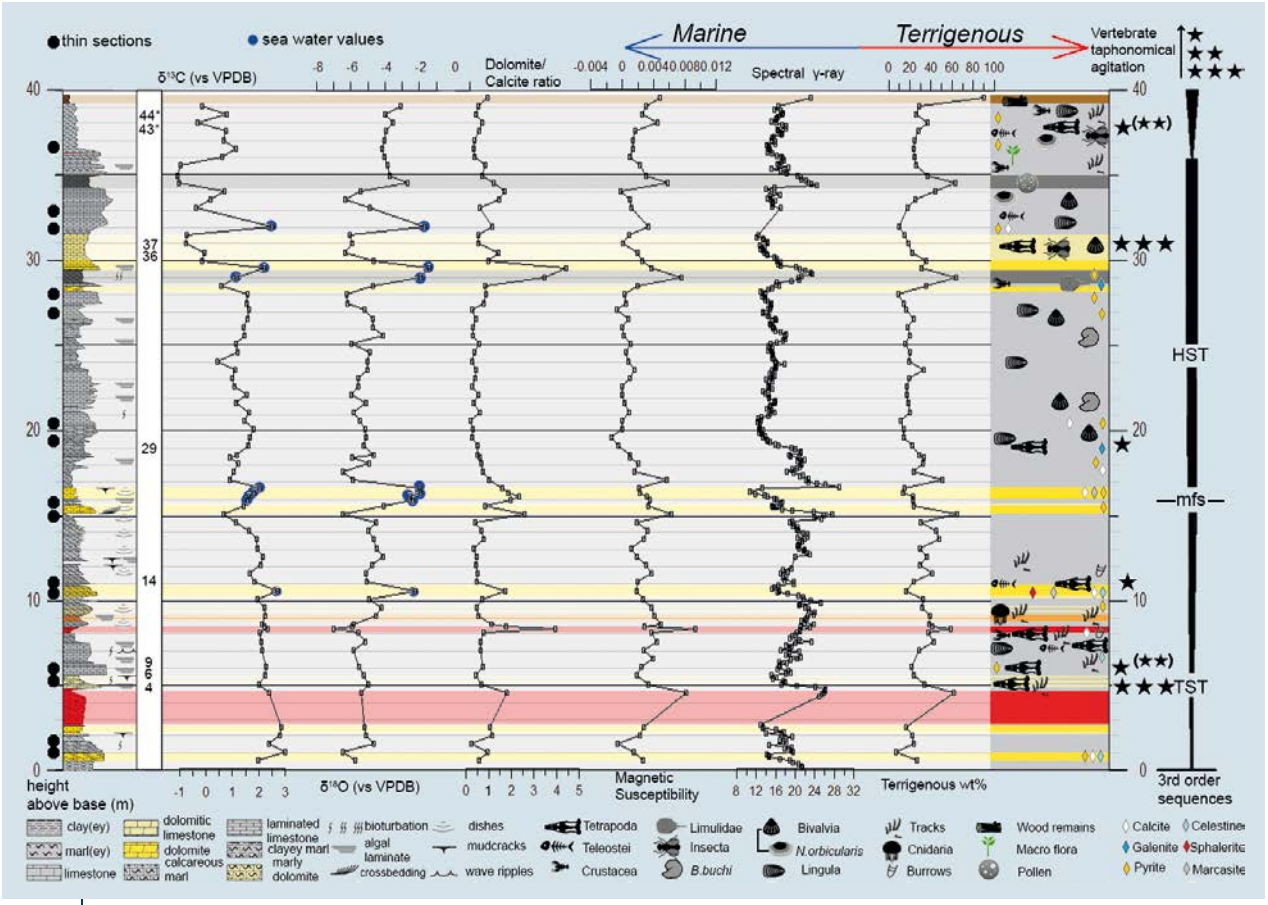

FIGURE 1. | *From left to right: Thin section sampling locations, statigraphic column modified after Pietersen (2010), fossiliferous layers after Oosterink (1986), $\delta^{13}C$ vs VPDB, $\delta^{18}O$ vs VPDB, dolomite/calcite ratio, magnetic susceptibility (in SI units $*10^{-9}$) and spectral γ-ray by Pietersen (2010), lithogenic wt% TGA, fossil and mineral occurrences, taphonomic agitation (1-3 stars corresponds to intensive- light reworking, vertebrate taphonomy declared between brackets indicate occasional variability in taphonomy), and the third-order sequences after Diedrich (2001). Abbreviations: TST: Transgressive System Tract, MFZ: Maximum Flooding Zone, HST: Highstand System Tract. Arrows indicate more marine (left) and more terrigenous (right) depositional conditions.*

to form the epicontinental Muschelkalk Sea (Aigner, 1985). The flooded continental lowlands accommodated the deposition of sediments in a shallow-to-moderately-deep marine environment, forming the Muschelkalk Formation. In the Winterswijkse Steengroeve, the Muschelkalk sequence is unconformably overlain by Rhaetian claystone of marine origin. As neither the Muschelkalk nor the Rhaetian claystone contain material that is suitable for radiometric dating, all ages are based on litho/biostratigraphical correlations with radiometrically dated sections.

The Vossenveld Formation that crops out in the Winterswijkse Steengroeve corresponds to the Lower Muschelkalk Wellenkalk facies and was deposited during Anisian (Bythinian, Pelsonian, and earliest Illyrian) times (Hagdorn & Simons, 2010); between ~246 and ~243 million years ago (Ma). It preserves coastal and near-shore sediments of the Muschelkalk Sea situated approximately 14° north of the equator (Ziegler, 1999; Dülfer & Klein, 2006; van Hinsbergen *et al*., 2019). The overall transgressive records of the Vossenveld Formation primarily consist of micritic limestones of microbial origin (Borkhataria *et al*., 2006; Geluk, 2007). Numerous beds within this succession preserve a diverse shallow marine faunal assemblage encompassing reptiles, fishes, and invertebrates such as crustaceans, medusozoan Cnidaria (e.g. jellyfish), and bivalves (e.g. Rieppel, 2000; Albers *et al*., 2003; Oosterink *et al*., 2003; Hauschke *et al*., 2009; Oosterink & Winkelhorst, 2013; Klein & Scheyer, 2014; Voeten *et al*., 2015; Maxwell *et al*., 2016). The tetrapod assemblage of these deposits is known through skeletal material and coprolites of sauropterygians and trackways from terrestrial reptiles (e.g. Schulp *et al*., 2017; Marchetti *et al*., this volume page 250).

The Vossenveld Formation is particularly known for its sauropterygian diversity that includes the endemic taxa *Lariosaurus vosseveldensis, Lariosaurus winkelhorsti, Pararcus diepenbroeki*, and *Palatodonta bleekeri* (e.g. Klein *et al*., 2016; Lin *et al*., 2017). Besides sauropterygians, other tetrapods such as the prolacertiform *Amotosaurus rotfeldensis* (Wild & Oosterink, 1984, but also consider Spiekman *et al*., this volume page 208), ?*Eusaurosphargis* (Sander *et al*., 2014; Klein & Sichelschmidt, 2014), and amphibians are known from this locality. Various fish taxa are represented (e.g. Oosterink *et al*., 2003), and even introduced remains of insects have been described (Van Eldijk *et al*., 2017). Body fossils of vertebrates are usually preserved in three dimensions and despite the common hallmarks of taphonomic agitation (Heijne *et al*., 2019), skeletal elements typically retain their original morphological characteristics.

This work aims to shed more light on the depositional environment and faunal distribution of the Vossenveld Formation, with special attention to the environmental conditions that hosted the shallow marine paleo-assemblage and preserved the faunal remains in this environment shortly after the end-Permian extinction event.

Material and methods

Conventional sedimentological characteristics, such as lithology, texture, particle size, and erosional characteristics, were recorded during various sampling campaigns between 2006 and 2008 along the north-western wall of the quarry. Spectral γ-ray analyses were performed in situ in the quarry with an Exploranium GR-320 ENVIspec at a 10-cm-resolution. These measurements provide information on both the clay mineralogy and content by measuring the decay of potassium, uranium and thorium, as well as total γ-ray.

Physical rock samples were extracted approximately every 50 cm throughout the 40 m sequence. Magnetic susceptibility was measured with an AGICO KLY-2 KappaBridge at the Paleomagnetic Laboratory Fort Hoofddijk of Utrecht University (The Netherlands).

Thin sections were prepared for petrographic analysis using light microscopy; Zeiss Axioskop 2 and Leica DM2500M microscopes.

For whole-carbonate analyses, every rock sample was ground down in the Fritsch Pulverisette 2 mortar grinder, after which 2 g of the homogenised sample was weighed for thermogravimetric analysis (TGA) and ~0.3 mg of every sample for stable isotope analysis.

The samples for the TGA were dried in an oven at 60 °C, after which 2 g of material was transferred to a porcelain container and placed inside the LECO TGA 601 of the Sedimentological Laboratory (Earth Sciences, Vrije Universiteit, Amsterdam, the Netherlands). Sample temperature was raised in stages, and at each stage, weight loss due to decomposition was measured. This enables determination of the carbonate composition for each sample. Since $MgCO_3$ decomposes at temperatures ranging from ~725 to ~875 °C and $CaCO_3$ decomposes at temperatures ranging from ~875 to ~1000 °C (pers. comm. Kay Beets), raw TGA data could be interpolated to determine the dolomite content. The relative abundances of pure dolomite ($MgCa(CO_3)_2$) and pure calcite ($CaCO_3$) can subsequently be reconstructed by correcting for CO_2 loss using respectively formula 1 and formula 2:

$$\text{Dolomite wt\%} = \left(\frac{CO_{2(\text{grams})}}{44}\right) * \frac{100+84}{2}$$

Formula 1

$$\text{Calcite wt\%} = \left(\frac{CO_{2(\text{grams})}}{44}\right) * 100$$

Formula 2

Where $CO_{2\,(\text{grams})}$ is the weight of CO_2 loss in the temperature range of the respective carbonate, 44 g mol^{-1} is the molar mass of CO_2, 84 g mol^{-1} is the molar mass of $MgCO_3$ and 100 g mol^{-1} is the molar mass of $CaCO_3$. The abundance of calcite versus dolomite in bulk carbonate sediment is far higher, rendering it unlikely for the magnesium content to exceed the calcium content in dolomite. The average molecular weight for $MgCa(CO_3)_2$ was inferred following (100+84)/2 = 92 g mol^{-1}.

The stable oxygen and carbon isotopic compositions are expressed as the ratio of the rare isotope (^{18}O and ^{13}C, respectively) over the abundant isotope (^{16}O and ^{12}C, respectively) in the delta (δ) notation:

$$\delta = \left(\frac{\left[\frac{^{13}C}{^{12}C}\right]_{\text{sample}}}{\left[\frac{^{13}C}{^{12}C}\right]_{\text{standard}}} - 1 \right) * 1000$$

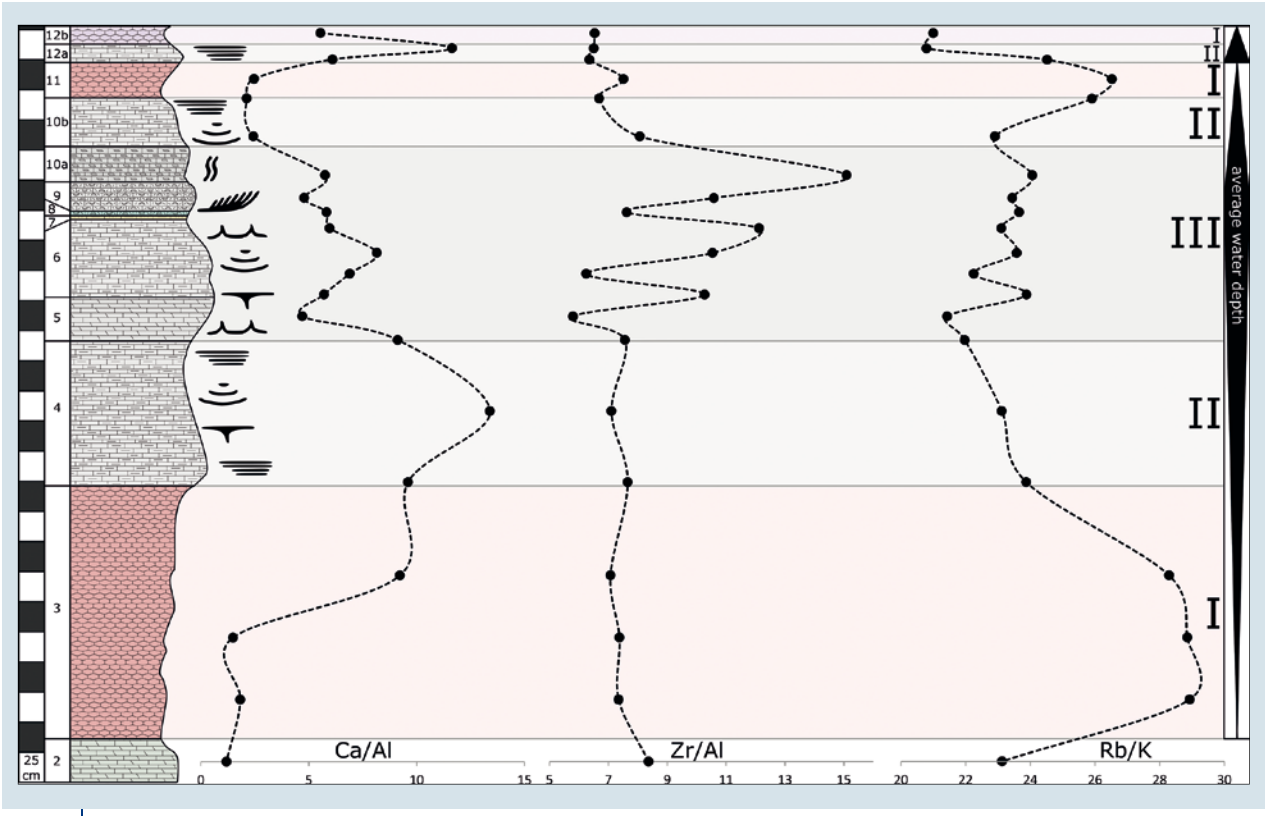

FIGURE 2. | *Fluctuating Ca/Al, Zr/Al, and Rb/K ratios along the transgressive-regressive stratigraphic interval of the Vossenveld Formation spanning layers 2 – 12 after Oosterink (1986). Layers 10 and 12 were subdivided in two distinct horizons following lithologic and textural differences observed during sampling. Sedimentary structures indicated using symbols used in Figure 1. Roman numerals on the right designate subfacies I – III, all within Facies 1 (Mudstones with halite pseudomorphs) identified through petrography. Transgressive-regressive intervals indicated through generalised average water depth. Element abundances in % (Ca, Al, and K) and ppm (Zr and Rb).*

For the stable oxygen and carbon isotopic compositions of bulk carbonate, samples were placed in Exetainer vials with pierceable endcaps and flushed with purified helium gas. Orthophosphoric acid was added thereafter and allowed to react for 24 hours at 45 °C to ensure complete dissolution of the dolomite fraction. Subsequently, the CO_2-He mixture samples were analysed with a Thermo Finnigan Delta-Plus mass spectrometer connected to a Thermo Finnigan GasBench II preparation device. Uncertainties for $\delta^{13}C$ and $\delta^{18}O$ were 0.19‰ and 0.23‰ respectively, as determined by multiple analyses of IAEA-CO-1 ($CaCO_3$ Carrara Marble carbonate standard) in the Stable Isotope Laboratory (Earth Sciences, Vrije Universiteit, Amsterdam). All isotopic compositions are expressed against the Vienna Pee Dee Belemnite (VPDB).

The $\delta^{18}O$ data allow for a tentative temperature reconstruction by application of the paleotemperature calculations from Craig (1965). This reconstruction is based on the $\delta^{18}O$ estimation of -2‰, VSMOW (Vienna Standard Mean Ocean Water) as suggested for Muschelkalk Sea conditions by Korte *et al.* (2005). As the temperature-dependent oxygen isotope fractionation factor varies between dolomite and calcite, the 2.6‰ correction as suggested by Vasconcelos *et al.* (2005) has been applied to the samples from the dolomite beds.

Rock samples spanning a basal interval (~6 m thick) of the Muschelkalk stratigraphy cropping out in the Winterswijkse Steengroeve, including a distinct transgression-regression cycle between presumed subaerial red marls, were prepared for XRF analysis, all at the Geochemical Laboratory (Vrije Universiteit, Amsterdam). The samples were dried overnight in a Heraeus drying oven at 110 °C and subsequently freed from eventual secondary surface mineralisations using a brass brush, as copper and zinc concentrations were not considered. The cleaned samples were crushed using a Fritsch jaw crusher and powdered using a Fritsch Pulverisette 5 planetary ball mill that were both cleaned with a paint brush and ethanol after each sample preparation. Circa 10 g of ground rock powder was dried once more at 110 °C. Exactly 4.5000 g of rock powder was mixed with 10% of sample weight in organic binder (EMU 120 FD; BASF) for 15 minutes with a mixing machine using agate balls. Powdered samples were subsequently transferred to Spec-Caps, covered with plastic film, and bound at 20 ton of compression for 45 seconds using a die plunger. The finished pellets were carefully removed from the pellet die set and subjected to XRF analysis. The concentration of several major and trace elements was determined for each pellet using the Philips MagiX PRO sequential spectrometer in 'Spell' configuration. Following sedimentological descriptions recorded during field sampling, sample points were correlated to and projected on their corresponding level within the generalised lithostratigraphic column of Oosterink (1986).

Results

The detailed lithostratigraphic column and geochemical and geophysical data (TGA bulk chemistry, magnetic susceptibility, spectral γ-ray, $\delta^{18}O$, and $\delta^{13}C$) are presented in Figure 1. The various limestones are indicated in gray, dolomites are colored yellow, red has been applied for the red marls, dark gray indicates clay beds, and the single brown layer at the top indicates the Rhaetian cover unconformably capping the Muschelkalk section. On average, the Vossenveld Formation has a lithogenic content (i.e. weathering products of bedrock and soils) of 32 weight percentage (wt%), with a standard deviation of 16 wt% (1 σ), ranging between 7 wt% and 90 wt% through the section. The total spectral γ-ray data have an average of 18 counts per second (cps; standard deviation is 3.3) and a range from 12 to 28 cps. The magnetic susceptibility data have an average value of 2 (standard deviation 2) with a range from 9 to -1 (in SI units $\star 10^{-9}$). The magnetic susceptibility curve yields a comparable pattern to the spectral γ-ray and lithogenic wt% curves. The lithogenic fraction distribution shows the same trends as magnetic susceptibility and spectral γ-ray, which have both been measured at a far higher resolution than the lithogenic wt%.

The dolomite/calcite ratio is considered 1 when a sample consists of 50% dolomite and 50% calcite. The average value for this ratio is 0.9 (standard deviation is 0.8), and it ranges between 0.2 and 4. The bulk Muschelkalk is therefore dominantly calcitic, yet major dolomitic layers are evidently present, such as the double dolomite banks at approximately 15-17 m (Fig. 1). The red marl beds at approximately 2.5-4.5 m and 8.0 m show a relatively large dolomitic fraction, coinciding with high values in magnetic susceptibility, spectral γ-ray, and lithogenic wt%.

The $\delta^{18}O$ data show an average value of -2.4‰ (standard deviation 0.1‰) and range from -7.0 to -1.4‰. The $\delta^{18}O$ curve generally peaks in the dolomite beds and dark clay beds (Fig. 1) and shows negative excursions in the red marls. The average $\delta^{13}C$ value is 2.5 ‰ (standard deviation 0.1‰), but varies between -1.1 and 3.0 ‰. A pattern comparable to that of the $\delta^{18}O$ curve can be seen in the $\delta^{13}C$ data, with peaks in the dolomite beds and negative excursions in the red marls. Opposing values occur in the dark clay layers, where the $\delta^{18}O$ values are relatively high and $\delta^{13}C$ values are low. The $\delta^{13}C$ curve exhibits a general decreasing trend through the stratigraphy whereas the $\delta^{18}O$ values generally increase.

Petrographic analysis

Based on petrographic analysis of the thin sections (positions indicated in the left margin of Figure 1), three main limestone facies can be recognised in the peritidal depositional system of the Vossenveld Formation at Winterswijk.

Facies 1: Mudstones with halite pseudomorphs (~0 – 10.5 m above base)

Description: Facies 1 is characterised by laminated calcareous mudstones that occasionally grade upwards into micro-ripple laminae. The micro ripples always occur entrapped as isolated features in the laminated mud. The mudstones are associated with abundant halite pseudomorphs and polygonal desiccation cracks (Fig. 4A & B). Apatite fragments (calcium phosphatic materials) occur randomly scattered and exhibit structures recognizable as skeletal fragments (Fig. 4B).

Facies 2: Micro cross-laminated mudstones (~11-20 m above base)

Description: Facies 2 is defined by laminated- to micro cross-laminated calcareous mudstones (Fig. 4C). Micro ripples are oppositely oriented and silt-sized quartz grains occur along the laminar surfaces. The silt is frequently concentrated in isolated lenticular bodies (1–2 mm in diameter) of carbonate mud (Fig. 4D) and appear to represent loaded rip-up clasts. The horizontal lamination is usually marked by the organisation of silt grains.

Facies 3: Microbial laminated mudstones (~20.5-36 m above base)

Description: Facies 3 shows an alternation of calcareous mud laminae and silt-rich laminae. This fine lamination laterally grades into a wavier bedding, which commonly contains either casts or pseudomorphs of evaporitic minerals such as gypsum (Fig. 4E).

XRF on the lower 6 meters

Petrographic analysis of Facies 1 (Mudstones with halite pseudomorphs) identifies three subfacies in the stratigraphic transgressive-regressive interval spanning layers 3–11 (Oosterink, 1986), which preserve distinct geochemical signatures characteristic for their genesis and post-depositional development (Fig. 2). Across various sedimentary rocks, ion exchange and differential adsorption during weathering causes the enrichment of rubidium (Rb) relative to potassium (K; Heier and Billings, 1970). Relative abundance of Rb (in ppm) over K (in % K2O), as obtained through XRF analysis, revealed that the Muschelkalk 'red marl beds' of Subfacies I are enriched in Rb relative to K. The supratidal to incidental intertidal micritic laminates of Subfacies II, preserving mud cracks and vertebrate trackways, exhibit lower Rb/K ratios. The same holds for the distal intertidal to subtidal interval of Subfacies III, including layer 9 that bears signs of agitation through the presence of rounded rip-up clasts and reworked skeletal elements. Nevertheless, the more obvious transitions to the thick and thin red marl beds might be associated with subaerial weathering, indicating either gradual bathymetric cycles or secondary mobility of its corresponding cation signatures into the more permeable marls.

Al-normalised Ca content (Ca/Al) offers a relative measure for the abundance of predominantly marine carbonates versus the terrigenous material, since Al is mainly present in aluminosilicates (i.e. mostly clay minerals; e.g. Riethdorf *et al*., 2013). The thickest interval representing Subfacies II (layer 4; Oosterink, 1986), but also the thin intercalation of Subfacies II in layer 12a, exhibit the highest Ca/Al ratios in the analysed subsection. This is consistent with microbial activity in the intertidal domain of Subfacies II representing the dominant source of lime mud constituting the local Muschelkalk matrix. Supportive evidence for this interpretation is offered by the presence of pitted surfaces in this domain. These semicircular depressions

FIGURE 3. | *Mud-crack laminate (Subfacies II) with pitted surface (negative) and puddle displaying gas bubbles. Note the lime-mud texture supporting collapsed bubble marks along the puddle margin. Geological hammer for scale.*

originated as collapsed gas bubbles resulting from cyanobacterial metabolic activity during shallow submersion of the substrate. The uptake of CO_2 for photosynthesis causes the precipitation of carbonate from the ambient seawater. This process mediated biochemically induced deposition of automicritic mud, with the gas bubbles trapped in calcareous ooze likely reflecting associated oxygen formation (Dupraz *et al*., 2009; Glunk *et al*., 2011) – a phenomenon that can be observed in ephemeral puddles in the quarry today (Fig. 3).

The proximal inter- to subtidal deposits of Subfacies III yields generally lower, less variable Ca/Al ratios than Subfacies II together with strongly fluctuating, moderate to high Zr/Al ratios. Zirconium is among the most abundant trace elements in terrestrial rocks and occurs predominantly in the mineral zircon (Milnes & Fitzpatrick, 1989), which has a high specific density of around 4.7 (Mursky & Thompson, 1958) and is among the most weathering-resistant minerals known (e.g. Dryden & Dryden, 1946). These properties allow for a relative concentration of zircon crystals in fluvial sediments while other minerals progressively break up and weather away (Key *et al*., 2012). A strongly fluctuating Zr/Al ratio in Subfacies III is consistent with episodic removal of the clay minerals by storm activity, transport, and redistribution of larger, heavier particles. This observation coincides with the relative concentration of skeletal elements in the environments represented by Subfacies III, most notably around layers 6–10a. Lower Ca/Al ratios around these levels indicate an overall more agitated depositional setting than those represented by Subfacies II, as Ca-rich automicritic lime mud appears to have been partially washed out by storm activity, thereby elevating the relative abundance of the more cohesive clay minerals that are richer in Al.

Distribution of diapsid taxa

Despite the potential of finding fossil remains throughout the stratigraphy, the highest concentrations of fossils are presently known from layers 4, 6, 9, 10, 14, 29, 36, 37, 43, and 44 (the last two were added after publication by Oosterink, 1986). The known stratigraphic distributions of ten recognized taxa (Fig. 6) are based on both literature and communications from private collectors from the Werkgroep Muschelkalk Winterswijk (Workgroup Muschelkalk Winterswijk). Material from *Tanystropheus* has been found in layers 9 and 29 (Spiekman *et al.,* in this volume) and from an unspecified horizon between these layers (Wild & Oosterink, 1984). Material from ?*Eusaurosphargis*, mostly comprising the characteristic vertebrae with long transverse processes, ribs with uncinate processes, and osteoderms, is generally rare but regularly encountered in e.g. layer 9 and layer 14. This taxon is also represented by several additional associated girdle- and appendicular elements recovered together with material from *Anarosaurus* and a pistosauroid between layer 4 and layer 9 (Sander *et al*., 2014). Notably, an ?*Eusaurosphargis* vertebra and putative osteoderm have been reported from layer 9 in association with an isolated dentary resembling that of the basal placodontiform *Palatodonta* (Willemse *et al*., this volume). *Saurosphargis*/*Paraplacodus* was reported from the Vossenveld Formation (Oosterink, 2003), although this identification remains tentative. The single recorded occurrence of *Palatodonta bleekeri*, which is also the only species in this genus and argued to be indicative of a European origin of Placodontiformes (Neenan *et al*., 2013), was reported from layer 9. Placodonts, however, are far more common higher in the stratigraphy, where representatives also attain notably larger body sizes. Remains of *Placodus* have

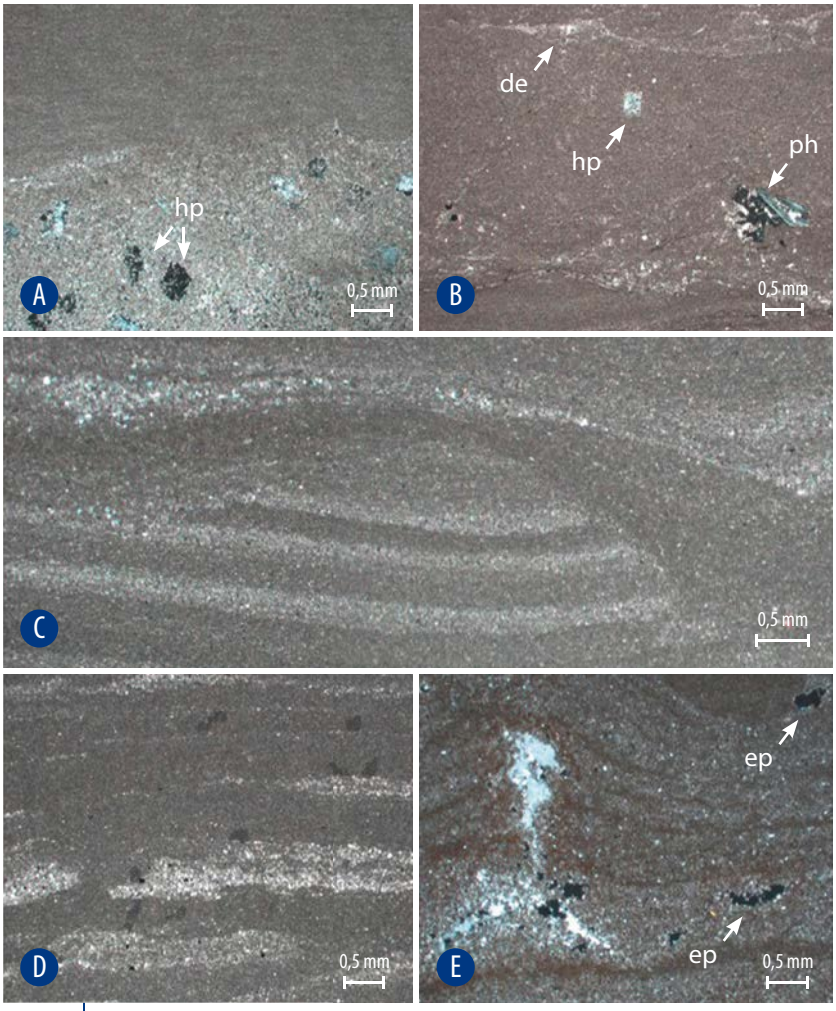

FIGURE 4 | *Photomicrographs of sedimentological features preserved in the Vossenveld Formation. (A) and (B): Thin sections of fine-grained mudstone with halite pseudomorphs (hp), phosphatic fragment (ph) and desiccation cracks (de) with a pseudo–evaporitic infilling (arrow) of Facies 1. (C): Micro cross-laminated mudstone with upwarps and low angle, curved intersections of Facies 2. (D): Lenticular fine-grained silt bodies isolated in mudstone matrix of Facies 2. (E): Microbial laminae appearing as crinkled, multi-layered mats with pseudo–evaporatic crystals (ep) of Facies 3.*

been found in layers 36 up to the hypersaline layer 44, yet are entirely absent in the lowermost 31 m of the Vossenveld Formation (Bickelmann & Sander, 2008; Klein & Scheyer, 2014; Voeten *et al*., 2015; During *et al*., 2017). The so far endemic species *Pararcus diepenbroeki* has been recognized in three individual finds from layer 14 up to layer 37 (Klein & Scheyer, 2014; During *et al*., 2017). Another placodont recovered from the Vossenveld Formation is a likely cyamodontoid (armored) placodont that was encountered in layer 9 (Albers, 2005). The only pachypleurosaurian genus known from Winterswijk is *Anarosaurus*, which has been found throughout the stratigraphy (e.g. Rieppel & Kebang, 1995; Oosterink *et al*., 2003; Klein, 2009; Klein & Sander, 2019;). Similar to *Anarosaurus*, the apex predator of the Anisian Muschelkalk Sea, *Nothosaurus*, too has been found throughout the stratigraphy and notably increases in size upwards along the stratigraphy, although the largest material could also belong to ?*Cymatosaurus* (e.g. Oosterink, 1986; Lankamp, 2002; Albers & Rieppel, 2003; Bickelmann & Sander, 2008; Klein & Albers, 2009; Voeten *et al*., 2015). Contrary to *Anarosaurus* and *Nothosaurus*, the finds of *Lariosaurus vosseveldensis* and *Lariosaurus winkelhorsti* (until recently *Nothosaurus winkelhorsti*: Lin *et al*., 2017) are restricted to layer 9 (Klein & Albers, 2009; Klein *et al*., 2016). Finally, basal pistosauroid bones have been described from the lower regions of the stratigraphy (Sander *et al*., 2014; Voeten *et al*., 2015).

Discussion

During the deposition of the Vossenveld Formation, the region of Winterswijk was a proximal tidal flat with shallow yet fluctuating and generally increasing water depths, which is reflected in the sequential deposition of marls, limestone, dolomite, and clay. Although transgressive and regressive episodes alternate throughout the section, causing substantial variability in water depth, the overall relative rise in sea level was recognised as an overarching third-order sequence (Diedrich, 2001). The occurrence of terrestrial vertebrate trackways, as well as swimming traces, only centimetres above winnowed bonebeds (Aigner, 1982; Aigner, 1985; Schulp *et al*., 2017), indicate that relative sea-level variability was evident and that local storm reworking occurred. The influx of lithogenic particles likely reflects aeolian introduction of terrigenous particles from the adjacent hinterland. These particles are most abundant in the red marls and dark clay beds, where the carbonate content is low (Fig. 1). The relatively lower carbonate background sedimentation could also allow for the relative enrichment in terrigenous components in contrast to increased dilution during episodes of higher carbonate precipitation. Depositional conditions varied from relative deep-water conditions to sub-aerial conditions. This is recorded as fluctuations in the aeolian transport of terrigenous material and in the dolomite/calcite ratio.

There are two main processes of dolomite formation: 1) dolomitization, replacement of $CaCO_3$ by $CaMg(CO_3)_2$, and 2) dolomite cementation (precipitation), where dolomite precipitates from an aqueous solution (Machel, 2004). Dolomitization is a secondary formation of dolomite via diagenesis, contrarily dolomite precipitation is a primary formation of dolomite, which is quite rare today as it requires e.g. lagoonal shallow settings with high evaporative rates. On the other hand, dolomitization usually occurs as sea water is 'pumped' through carbonate sequences at temperatures of ~50-80 °C (Machel, 2004). In the Vossenveld Formation, the dolomite facies appear to be formed under shallow marine, evaporative conditions, with higher salinity and/or under higher temperatures than the calcium carbonate

precipitation. The marine $\delta^{18}O$ values observed in the dolomite facies (Fig. 1) further reinforce the likeliness that the dolomite was primarily precipitated from the shallow sea water. Although the possibility of early secondary dolomitization may not be excluded, the basinward increasing salinity (Szulc, 2000) combined with the preservation of marine $\delta^{18}O$ values, suggest a primary origin of dolomite (Machel, 2004; Clark & Fritz, 1997). Although it cannot be excluded that secondary dolomitization played a role elsewhere, primary dolomitization appears to have formed the majority of the dolomite banks in the Vossenveld Formation. The high oxygen isotope values occurring at the two thick dolomite banks at ~15 m above base might be linked across the Germanic Basin, coinciding with the maximum flooding zone recognized in Northern Switzerland, Central Germany and Southern Poland (Feist-Burkhardt *et al*., 2008), possibly resulting from a marine incursion.

Depositional environment

Limestone facies predominate in the Vossenveld Formation and contain most, if not all, vertebrate fossil remains. In this study, the petrographic study of thin sections identified three types of limestone facies:

Facies 1: represents depositional settings analogue to brine pools or a coastal sabkha that are predominantly present in the supratidal zone. The presence of halite observed in desiccation cracks indicates generally arid conditions in a depositional system that is strongly influenced by periodic marine flooding.

Facies 2: contains oppositely-oriented ripple marks that could have been caused by a weak tidal activity or seasonal and/or episodic storm-driven currents in a shallow-gradient coastal setting.

Facies 3: contains features that are indicative of stratiform microbial sheets, which are formed in the intertidal zone almost completely sheltered from wave actions. The occurrence of crypto-algal mats and evaporitic minerals further supports highly evaporative conditions and are associated with supersaturated marine waters.

The succession of the Vossenveld Formation records an overall transgressive environmental shift from the supratidal to the intertidal zone over time. The occurrence of halite and polygonal desiccation cracks in association with supratidal mud further indicates that fresh-water runoff onto the tidal flats was low or entirely absent. Opposingly orientated cross laminations offer some evidence of tidal-like activity, although this influence was very weak. The occurrence of stratiform crypto-algal sheets in association with evaporitic minerals is typical for shorelines protected from agitating wave activity, although tidal activity might have allowed the microbial mats to flourish. The tidal influence on sediment reworking was possibly reduced by stabilization of the sediment surface by algal mats. The shielded nature of the local environment might have been further attributed to the shallow bathymetry and enclosed nature of the Muschelkalk Sea in general. Low facies diversity and the gradual transition from supratidal to intertidal facies indicate that local variations in topography strongly influenced the sedimentation pattern, which is observed laterally throughout the quarry outcrops and bedding planes preserving terrestrial footprints and swimming traces near each other. The temporal facies change indicates that the depositional environment developed in response to a large-scale marine transgression, which is in line with decreasing $\delta^{13}C$ and $\delta^{18}O$ values.

Some limestones experienced a considerable degree of karstification, particularly in the upper 5 m (Oosterink *et al*., 2006), as can be recognized in the deviating stable isotope records. During karstification, rainwater percolates through the strata while dissolving and re-precipitating calcium carbonate, which could alter the isotopic signal of the calcium carbonate. Diagenetic effects on the isotope signatures of marine carbonates have the potential to complicate paleoclimatic reconstructions (Edgar *et al*., 2015). Meteoric diagenesis, by interaction with freshwater (rain and pore water), can dramatically lower the stable oxygen and carbon isotope composition of the bulk sediment (James & Choquette, 1984; Moore, 1989; Moore, 2001; Bishop *et al*., 2014).

Paleoenvironment

Within the lithostratigraphy of the Winterswijkse Steengroeve we find marls, dolomites, limestones and clays. As the thin sections were limited to the limestones, three limestone facies could be identified in the petrographic study. Furthermore, three subfacies, not limited to the limestones, are identified in the basal 6 m of the stratigraphy through XRF.

The Lower Muschelkalk interval exposed in the Winterswijkse Steengroeve contains a ~3 m-thick calcareous micritic and marly stack sandwiched between two conspicuous reddish-brown clayey marl deposits (Subfacies I in Figure 2) that appear to have experienced substantial subaerial weathering. These red marl beds are nodular in appearance in the outcrop with poor expression of primary sedimentary patterns. Bathymetrical evolution from the thick (lower) to the thin (upper) red marl bed represents a single transgressive-regressive chapter within the section (e.g. Diedrich, 2001).

Subfacies II (Fig. 2) is represented by 'mud-crack marls' consisting of laminated light-gray calcareous mudstones with a layer thickness of a few millimetres to centimetres. These laminated mudstones often form hexagonal plates separated by sediment-filled mud cracks that propagate and diverge upwards, causing increasingly smaller dishes with more pronounced upwarped margins. Bedding planes preserve abundant tetrapod trackways that, alongside desiccation cracks, indicate episodic subaerial exposure. Certain horizons are richly populated with small hemispherical pits (Fig. 3).

A third, more heterogeneous subfacies (Subfacies III) encompasses laminated intertidal laminates as well as commonly to continuously submerged deposits. Subfacies III contains the fossiliferous layer 9 (Oosterink, 1986) that is characterized by the presence of typically isolated skeletal remains, crossbedding, and flattened rip-up clasts. Layer 9, interpreted as a tempestitic lag deposit (i.e. storm deposit; Voeten *et al*., 2015), shows substantial lateral variation in thickness, texture, and sedimentary structures throughout the quarry. Layer 9 overlies a

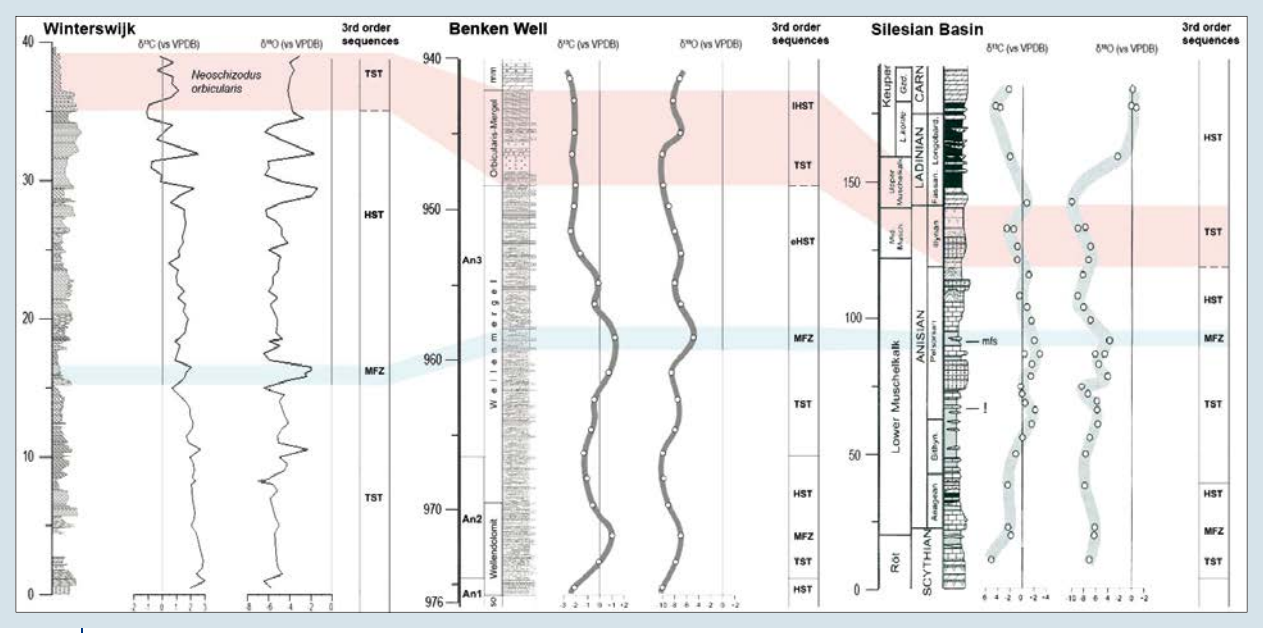

FIGURE 5. | *Tentative correlation between Lower to lower Middle Muschelkalk intervals in Winterswijk (the Netherlands), Benken (Switzerland), and the Silesian Basin (Poland) Abbreviations: TST: Transgressive System tract, HST: Highstand System Tract, lHST: late Highstand System Tract, eHST; early Highstand Systems Tract, MFZ; Maximum Flooding Zone. Dashed line represents a sequence boundary. View the original image at http://www.geologienederland.nl > Grondboor & Hamer > Staringia 16 for more details.*

thin, conspicuously green-colored erosional base layer enriched in skeletal remains, and is covered by an irregularly stratified bed, rich in *Rhizocorallium* burrows.

The bathymetric distribution of the subfacies presented here is described in terms of a 'tidal' range, although the enclosed and generally shallow nature of the Germanic Basin limits the influence of true (gravitational) tidality on the Muschelkalk Sea. It is proposed that the shallow to locally negligible gradient of the coastal setting predominantly supported storm-driven sea-level perturbations on sub-diurnal to seasonal time scales (i.e. Aigner, 1982; Borkhataria *et al*., 2006. All subfacies reported here were deposited along the shores and in the shallowest marine domains of a relatively arid sabkha environment analogous to the modern Persian Gulf (e.g. Schulp *et al*., 2017).

Correlation through isotope composition

As mentioned before, the Vossenveld Formation at the Winterswijkse Steengroeve is a highly fossiliferous deposit with remarkably good preservation. Nevertheless, most fossils do bear the signs of transport, indicating that the material was introduced post-mortem by occasional storm activity (Klein *et al*., 2015; Heijne *et al*., 2019). These features strongly suggest that the Anisian paleoenvironments recorded in Winterswijk do not necessarily reflect the environment in which marine reptiles spent most of their life, but opens the possibility that they resided in nearby regions with deeper water conditions (Klein *et al*., 2015). Nevertheless, since some bone material preserves post-mortem bite marks (Lankamp, 2002), marine reptiles likely resided in proximity (Klein *et al*., 2015) and may have at least occasionally entered the intertidal zone.

The stable isotope signature of the sediments of the Vossenveld Formation in the Winterswijkse Steengroeve, combined with petrographic and bio-stratigraphic information, allows for a tentative correlation with equivalent data retrieved from Muschelkalk sections further East and Southeast in the Germanic Basin (Fig. 5), e.g. the Benken Well by Feist-Burkhardt *et al*. (2008; Benken, Switzerland) and the Silesian Basin by Szulc (2000; Poland). Diedrich (2001) offered a stratigraphic interpretation of the Winterswijk Muschelkalk succession that includes a third-order sequence assignment (originally interpreted as a fourth-order sequence). Although section scaling and stage identification in Diedrich (2001) need re-evaluation, the overall relative sea-level fluctuations along the section appear correct and can be therefore used for basin-wide linkages.

Positive shifts in the $\delta^{13}C$ and $\delta^{18}O$ curves at circa 16 m in the Winterswijk section (MFZ according to Diedrich, 2001) mirror those at the mid-Wellenmergel and mid-Pelsonian maximum flooding zones of Switzerland and Poland. At ~ 35 m in Winterswijk, two opposing excursions in the $\delta^{13}C$ and $\delta^{18}O$ curves mark a distinct sequence boundary, above which hypersaline conditions prevail, as indicated by pseudomorph presence in the thin section (Fig. 4E), and the dominant occurrence of *Neoschizodus orbicularis* (Szulc, 2000; Röhling, 2002; Feist-Burkhardt *et al*., 2008). In Switzerland and Poland, comparable successions in which sediments deposited during a Lower Muschelkalk highstand stage are discordantly covered by hypersaline Middle Muschelkalk deposits of Illyrian age, corresponding to the Orbicularis Mergel.

This preliminary interpretation suggests that the Muschelkalk section in Winterswijk is predominantly Pelsonian in age, while the uppermost 5 m was

deposited during the Illyrian. As the lower portion of the Winterswijk section lacks convincing correlatable phenomena, this interval cannot be stratigraphically linked with other sections. Kozur and Bachman (2008) propose an age of 243.9 Ma for the Middle Muschelkalk sequence boundary. The proposed duration of the 3rd order cycles is as follows: the Lower Muschelkalk transgressive system tract (TST) lasted 0.6 Ma, while the Lower Muschelkalk highstand system tract (HST) and the Middle Muschelkalk TST both lasted 1 Ma, respectively (Calvet *et al*., 2009). Although strong lateral lithological variation, inferred variable sedimentation rates, and intervals of non-depositional regression and erosion could obscure precise durations, these dates suggest that the Muschelkalk section preserved in the Winterswijkse Steengroeve spans > 1 Ma, and potentially >2 Ma in total.

Figure 6 represents a chronostratigraphic overview reflecting the distribution of diapsid taxa, the estimated water temperatures, and a tentative estimate of the age of the deposit. Within the Vossenveld Formation, the best-known and most frequently searched fossil-bearing bed is layer 9 (Oosterink, 1986), from which, consequently, the most taxa are known. Notable sauropterygian trends along the Winterswijk section include an increase in average body size, as the strata higher in the stratigraphy appear to preserve larger specimens of *Nothosaurus* and placodonts (Oosterink, 1986; Bickelmann & Sander, 2008; Voeten *et al*., 2015). Obligate durophagous sauropterygians (i.e. *Placodus*) seem to be restricted to the higher stratigraphic intervals. For instance, *Palatodonta bleekeri* in layer 9 did not feature the specialised crushing dentition that *Placodus* had (Neenan *et al*., 2013). The presence of durophagous sauropterygians in the uppermost 10 m of the stratigraphy coincides with a higher abundance of bivalve-rich layers (Fig. 1), which suggests enhanced trophic opportunities for durophagous predators.

Despite the regular occurrence of vertebrate fossils and even insect remains (Van Eldijk *et al*., 2017), calcareous invertebrate body fossils are rare in the Vossenveld Formation. Their 'Steinkern' (i.e. moulds) preservation can be explained by aragonite dissolution

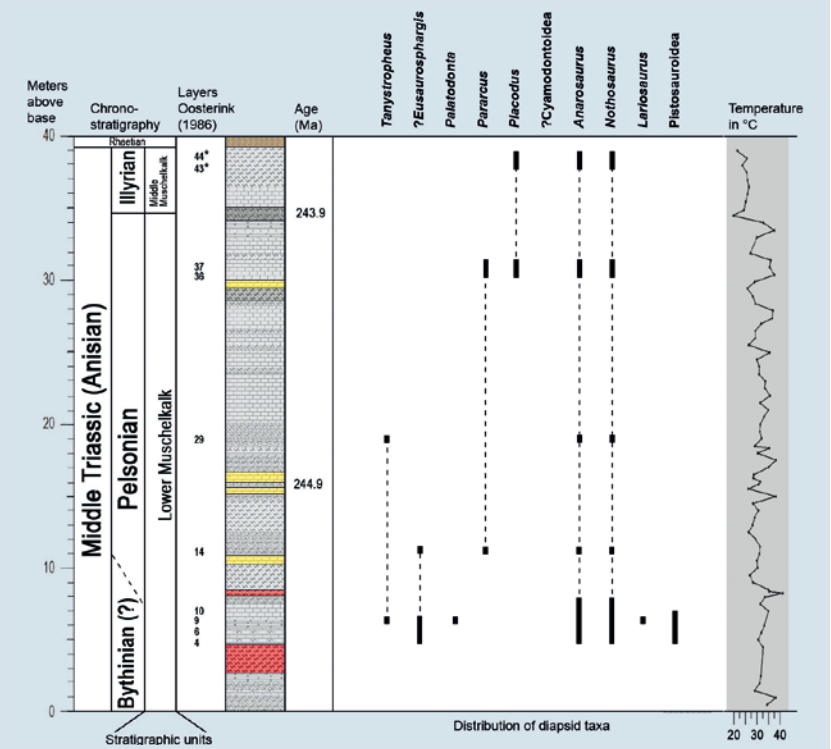

FIGURE 6. | *Chronostratigraphy and distribution of diapsid taxa in the Vossenveld Formation, with an indication of their known provenance layers (after Oosterink, 1986). Asterisk (*) = layers that have been added after the publication by Oosterink (1986). Temperature estimations follow Craig (1965) with corrections for dolomite suggested by Vasconcelos et al. (2005). Age estimates from Kozur and Bachman (2008) combined with the duration of the Highstand Systems Tract by Calvet* et al. *(2009).*

(Dertien & Dertien-te Voortwis, 1975; Klompmaker, this volume page 191). The thus-far identified invertebrate taxa (Fig. 1) include *Beneckeia buchi*, a ceratitic ammonoid (Diedrich, 2001; Oosterink, 2003) that occurs between ~20 m and ~28 m above the base of the section. It was recognised in limestones formed under relative deep-water conditions. The halophytic bivalve *Neoschizodus orbicularis* (Diedrich, 2001) is abundant in several distinct bivalve beds in the uppermost ~5 m of the Vossenveld section exposed in the Winterswijkse Steengroeve. In outcrops in northern Germany and the cored Benken well in northern Switzerland, the 'Orbicularis Mergel' is recognised through the frequent occurrence of this species. The Orbicularis Mergel represents an ecologically impoverished deposit and is considered part of the transitional sequence from the normal marine Lower Muschelkalk to the saline Middle Muschelkalk (Röhling, 2002; Feist-Burkhardt *et al*., 2008). The Middle Muschelkalk was deposited during a salinity crisis caused by a temporarily reduced hydrological connection between the Muschelkalk Sea and the Tethys Ocean, and its deposits are rich in evaporites (Szulc, 2000; Feist-Burkhardt *et al*., 2008).

Conclusions

During early to late Anisian times, sediments were deposited in an arid hypersaline sabkha environment along the western coastal region of the Muschelkalk Sea. These deposits are preserved in the Vossenveld Formation that crops out in the Winterswijkse Steengroeve. We studied geochemical and sedimentological proxies to provide environmental and paleoclimatological constraints for these Anisian tidal flats. These proxies offer informative tools that motivated a tentative correlation of the Vossenveld Formation with the Muschelkalk stratigraphy eastward in the Germanic Basin.

The episodically flooded tidal flats hosted extensive microbially-induced calcium carbonate precipitation. Microbial dolomite formation was likely governed by the influences of increasing temperature and rising salinity levels. Terrestrial

tetrapods trotted the tidal flats during brief episodes of subaerial exposure while longer periods of subaerial exposure caused alteration of the dolomites or limestones into oxidized red marls. The dark clays were not adequately sampled in this study to allow for extensive examination, yet their lighter carbon isotope signatures suggest phases of anoxia and increased sulphate reduction. The red marls exhibit strong and variable diagenetic alteration, which is likely a result of weathering upon subaerial exposure. This is corroborated by distinct geochemical indications for weathering. More recent meteoric diagenesis affected certain limestone intervals, particularly in the upper five metres of the section, which has affected the stable isotopic composition of the matrix. Recurring storm activity drove the influx of the skeletal body fossils, isolating and occasionally abrading these elements in the process. The adhesive nature of the automicritic ooze likely contributed to the concentration of three-dimensionally preserved fossil remains. The upper ~25 m of the Vossenveld Formation in Winterswijk are constrained to the Pelsonian and Illyrian substages of the Anisian. Finally, the composition of the diapsid assemblage along the section has been plotted to reveal ecological shifts that occurred only ~7 million years after the end-Permian extinction.

Acknowledgements

We would like to thank the late Henk Oosterink for all the work he has done, allowing us to further explore this remarkable chapter in Earth's history. The Werkgroep Muschelkalk Winterswijk, and specifically Herman Winkelhorst, Jos Lankamp, Gerard Goris, Remco Bleeker and Richard the Haan, are thanked for donating fossil material and sharing valuable information on the stratigraphic occurrence of fossil taxa. Sibelco Europe Minerals Winterswijk and its plant manager Gerard ten Dolle are acknowledged for allowing regulated access to their premises. Further thanks go out to Martine Hagen and Koos de Jong (VU Amsterdam) for conducting the TGA. Kay Beets and Mónica Sánchez Román (VU Amsterdam) kindly assisted in the interpretation of the data. Finally, we would like to thank reviewer Grzegorz Niedźwiedzki for his helpful comments and suggestions.

Samenvatting

De Winterswijkse Steengroeve in het oosten van Nederland ontsluit een ~40 m dik kalksteenpakket uit het Anisien (Trias) dat onder fluctuerende waterdiepte is afgezet. Hier presenteren wij een gedetailleerde stratigrafische beschrijving alsmede geochemische meetgegevens van het gesteente. Met behulp van stabiele isotopen werden paleotemperaturen van 25 tot 35 °C gereconstrueerd. Deze hoge temperaturen, op ~14° noorderbreedte, in combinatie met het afgesloten karakter van het ondiepe bekken, wijzen op hoge verdamping en een waarschijnlijk zeer zout milieu. De concentratie van losse skeletdelen en botten is een resultaat van stormactiviteit. Onverwacht is de toenemende saliniteit in de bovenste 10 m van de kolom, waar tevens grotere Sauropterygia en de zoutminnende tweekleppige *Neoschizodus orbicularis* voorkomen. Tevens is het stratigrafisch voorkomen van verschillende Sauropterygia geïnventariseerd, tezamen met een reconstructie van de condities waaronder ze zijn begraven en gefossiliseerd. De gecombineerde isotopen-, geochemische- en sedimentologische studie van de Vossenveld Formatie geeft meer inzicht in het milieu waarin de rijke fossiele assemblage van Winterswijk bewaard is gebleven. Dit nieuwe overzicht brengt ons weer een stap dichterbij het begrijpen van het biotische herstel na de Perm-Trias massa-uitsterving.

REFERENCES

- **Aigner, T., 1985.** *An ancient storm depositional system: Dynamic stratigraphy of intracratonic carbonates, Upper Muschelkalk (Middle Triassic), South-German Basin. Storm Depositional Systems: Dynamic Stratigraphy in Modern and Ancient Shallow-Marine Sequences, pp. 51-158.*

- **Feist-Burkhardt, S., A.E. Götz, K. Ruckwied & J.W. Russell, 2008.** *Palynofacies patterns, acritarch diversity and stable isotope signatures in the Lower Muschelkalk (Middle Triassic) of N Switzerland: evidence of third-order cyclicity. Swiss Journal of Geosciences, 101(1), pp. 1-15.*

- **Heijne, J., N. Klein & P.M. Sander, 2019.** *The uniquely diverse taphonomy of the marine reptile skeletons (Sauropterygia) from the Lower Muschelkalk (Anisian) of Winterswijk, The Netherlands. PalZ, 93(1), pp. 69-92.*

- **van Hinsbergen, L.P.P., van Hinsbergen, D.J.J., Langereis, C.G., Dekkers, M.J., Zanderink, B., and Deenen, M.H.L., in press.** *Triassic (Anisian and Rhaetian) paleomagnetic poles from the Germanic Basin (Winterswijk, the Netherlands), Journal of Palaeogeography, 8,30 doi:10.1186/s42501-019-0046-2*

- **Korte, C., H.W. Kozur & J. Veizer, 2005.** *$\delta^{13}C$ and $\delta^{18}O$ values of Triassic brachiopods and carbonate rocks as proxies for coeval seawater and palaeotemperature. Palaeogeography, Palaeoclimatology, Palaeoecology, 226(3), pp. 287-306.*

- **Kozur, H.W., & G.W. Bachman, 2008.** *Updated correlation of the Germanic Triassic with the Tethyan scale and assigned numeric ages. Berichte der Geologischen Bundesanstalt, 76, p.p. 53-58.*

- **Lankamp, J., 2002.** *Bijtsporen op een sauriërbot uit Winterswijk. Grondboor & Hamer, 56, pp. 26-27.*

- **Oosterink, H.W., 1986.** *Winterswijk, Geologie Deel II. De Trias-periode (geologie, mineralen en fossielen). Wetenschappelijke Mededelingen van de Koninklijke Nederlandse Natuurhistorische Vereniging, (178).*

- **Oosterink, H.W., 1993.** *Geologische verschijnselen in de groeven van de Winterswijkse Muschelkalk. Grondboor & Hamer, pp. 47-1.*

- **Szulc, J., 2000.** *Middle Triassic evolution of the northern Peri-Tethys area as influenced by early opening of the Tethys Ocean. In Annales Societatis Geologorum Poloniae. Vol. 70, No. 1, pp. 1-48.*

The full list of references can be found at: http://www.geologienederland.nl > Grondboor & Hamer > Staringia 16.
De volledige literatuurlijst is te vinden op: http://www.geologienederland.nl > Grondboor & Hamer > Staringia 16